Extended Abstracts of the 2015 International Conference on Solid State Devices and Materials, Sapporo, 2015, pp710-711

Source/Drain Contact Engineering of Molybdenum Disulphide (MoS_2) Devices

Wei Sun Leong[1], Xin Luo[2,3], Yida Li[1], Khoong Hong Khoo[3], Su Ying Quek[2], and John T. L. Thong[1]

[1] Department of Electrical and Computer Engineering, National University of Singapore, Singapore 117583.
Phone: +65-6516-2270 E-mail: elettl@nus.edu.sg
[2] Department of Physics, Centre for Advanced 2D Materials and Graphene Research Centre, National University of Singapore, Singapore 117546.
[3] Institute of High Performance Computing, 1 Fusionopolis Way, #16-16 Connexis, Singapore 138632.

Abstract

In this paper, we report a technique that is both facile and CMOS-compatible to achieve very low resistance source/drain contacts to molybdenum disulfide (MoS_2) field-effect transistors. We show, using both experimental approaches and first principles calculations, that the use of treated-graphene as buffer layer at the metal-MoS_2 contact can significantly reduce the Schottky barrier height (SBH) at the interface, and the contact resistance by 20-fold. Instead of Fermi level pinning by metal-induced gap states for pure metal electrodes, the SBH at the metal-graphene-MoS_2 interface is determined by charge transfer and interface dipole. Furthermore, we optimize the metal-graphene interface through fabrication of "edge contacts" that consistently provide low contact resistance owing to stronger coupling between metal and graphene, rather than further reduction of SBH.

1. Introduction

The performance of MoS_2 field-effect transistors (FETs) is often limited by the large electrical resistance associated with the metal contacts to MoS_2. Several approaches attempting to address this critical issue include metal work function engineering [1], molecular and chloride doping [2-4]. However, the achievable contact resistance is still far from satisfactory. Here, we report a technique to fabricate high-performance MoS_2 transistors by using Ni-treated graphene as a contact interlayer to enhance the carrier injection from metal into MoS_2.

2. Fabrication of Low-Contact-Resistance MoS_2 FETs

Fig. 1 shows the key process flow to fabricate MoS_2 FETs with Ni-treated-graphene electrodes. A dry transfer process is used to ensure perfect graphene-MoS_2 interface, while the optimization of metal-graphene interface is realized by an metal-assisted etching treatment that generates multiple nano-sized pits in the graphene enclosed by zigzag edges (Fig. 2 & Fig. 3), which are expected to form covalent bonds with the subsequent nickel metallization, rather than weak van der Waals bonds, thus resulting in much smaller contact resistance (Fig. 4) [5].

3. Electrical Performance of our MoS_2 FETs

Fig. 5 shows a typical optical image of the MoS_2 FETs with transmission line measurement (TLM) structure that used in this work to extract the contact resistance, R_C. The fitted R_C for MoS_2 FETs with Ni-treated-graphene electrodes was found to be 260 Ω.µm and 460 Ω.µm at back-gate biases of 50 V and 0 V, respectively (Fig. 5), which is the best reported value to date and approaches that required for the silicon-based technology at the 22 nm node [6]. In addition, we fabricated on the same exfoliated MoS_2 strip an array of MoS_2 transistors with both Ni-MoS_2 and Ni-treated-graphene-MoS_2 contacts and compared their device performance. We found that the on-current at V_{DS} = 2 V and V_G = 50 V shows ~12-fold improvement (Fig. 6) and the field-effect mobility enhanced by 4.3-fold (21.7 versus 93.4 cm^2/V.s), respectively, as a result of reduced contact resistance (Fig. 7). Table 1 summarizes the electrical performance of our MoS_2 FETs with Ni-graphene electrodes presented in this work.

Using first principle calculations, we found that the contact enhancement is mainly due to the significantly smaller work function of the Ni-graphene electrode compared to pure Ni (Fig. 8), which reduces SBH. The SBH of the Ni-graphene-MoS_2 interface is determined by charge transfer and the resulting interface dipole between Ni-graphene and MoS_2. This is in contrast to Fermi level pinning by metal-induced gap states for pure Ni electrodes. Bonds formation between Ni and zigzag graphene edges are found to result in stronger coupling and hence leading to further R_C reduction.

3. Conclusions

This work provides an insight into how the contact resistance at the metal-MoS_2 interface can be engineered with the use of graphene as an interlayer, and can possibly bring the use of MoS_2 as a mainstream electronic material to the forefront.

Acknowledgements

This project is supported by grant R-263-000-A76-750 from the Faculty of Engineering, NUS and grant NRF-NRFF2013-07 from the National Research Foundation, Singapore.

References

[1] S. Das *et al.*, *Nano Lett.* **13** (2013) 3396. [2] H. Fang *et al.*, *Nano Lett.* **13** (2013) 1991. [3] Y. Du *et al.*, *EDL* **34** (2013) 1328. [4] L. Yang *et al.*, *Nano Lett.* **14** (2014) 6275. [5] W.S. Leong *et al.*, *ACS Nano* **8** (2014) 994. [6] ITRS. In *Process Integration, Devices, and Structures* (2013). [7] H. Liu *et al.*, *ACS Nano* **8** (2012) 1031. [8] W. Liu *et al.*, *IEDM* (2013) 400. [9] Y. Du *et al.*, *EDL* **35** (2014) 599.

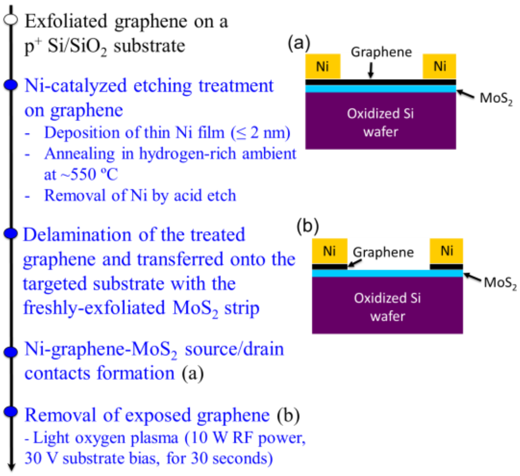

Fig. 1 Top-down process flow to fabricate MoS_2 FETs with Ni-graphene electrodes. Schematics of the device structure (a) prior to and (b) after the removal of exposed graphene on the effective channel regime.

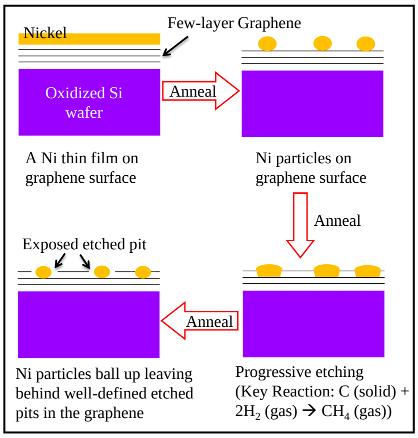

Fig. 2 Schematics illustrating the formation of well-defined etched pits in the few-layer graphene by the proposed Ni-catalyzed etching treatment.

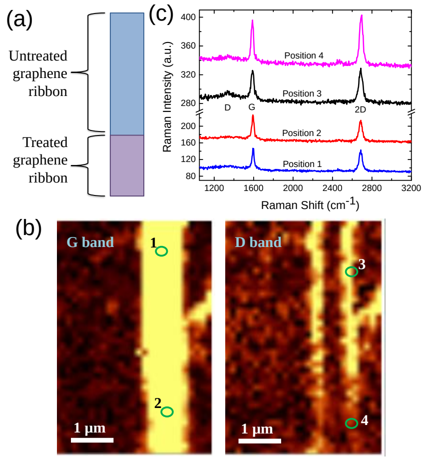

Fig. 3 (a) Schematic of a graphene ribbon defined by oxygen plasma and then partially treated with Ni-mediated etching. (b) Raman maps showing the intensity of the G- and D-band of the partially treated graphene ribbon. (c) Raman spectrum taken at the positions indicated in b.

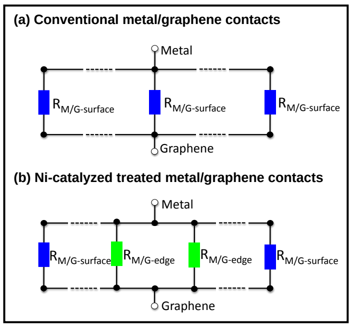

Fig. 4 Resistor network models comparison. It should be noted that $R_{M/G\text{-}edge} << R_{M/G\text{-}surface}$.

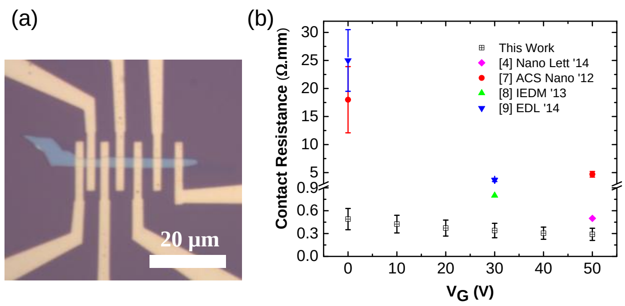

Fig. 5 (a) Optical image showing an array of MoS_2 FETs with Ni-graphene electrodes. The channel lengths varying from 0.5 to 3 μm, in steps of 0.5 μm. (b) R_C as a function of V_G. The R_C reported by others for MoS_2 FETs are included for comparison.

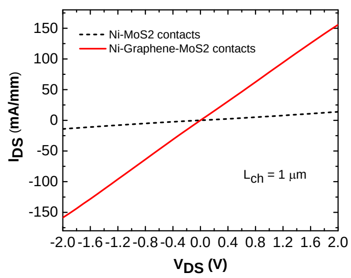

Fig. 6 I_D-V_D characteristics of MoS_2 FETs with and without the treated graphene as a contact interlayer (V_G = 50 V).

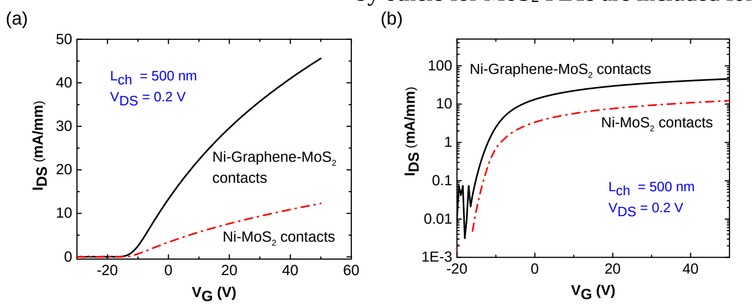

Fig. 7 Comparison of I_D-V_G characteristics for both MoS_2 FETs with and without the treated graphene as a contact interlayer that were fabricated on the same MoS_2 flake in (a) linear and (b) logarithmic scale.

Summary of MoS_2 FETs with Ni-graphene electrodes presented in this work	
L_{ch}	500 nm
R_c when V_G = 50 V	0.29 Ω.mm
I_{DS} when V_{DS} = 2 V	403 mA/mm
I_{ON}/I_{OFF} when V_{DS} = 0.2 V	10^5
μ_{FE}	93.4 cm²/V.s

Table 1. Summary of key parameter metrics of our MoS_2 FETs with Ni-graphene electrodes.

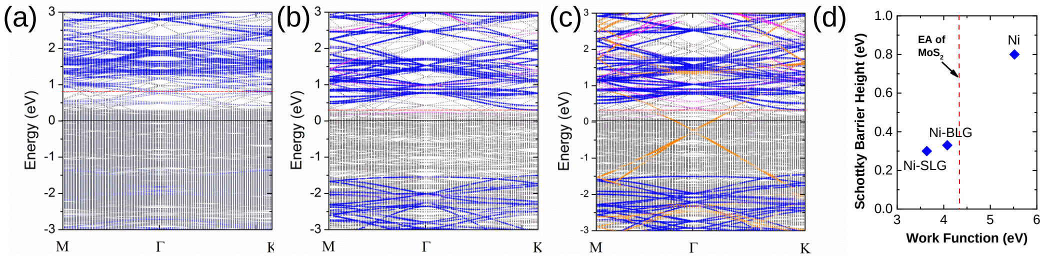

Fig. 8 (a) Band structures of single layer MoS_2 interfaced with (a) Ni, (b) Ni-SLG, and (c) Ni-BLG, only the minority bands are shown here for magnetic systems. The blue, pink and orange dots represent the projected bands of MoS_2, graphene layer close to Ni, and graphene layer adjacent to MoS_2 respectively, with the projection weight indicated by the dot size. The black solid and red dashed lines show the positions of the Fermi level and conduction band minimum of MoS_2 respectively. (d) SBH as a function of the electrode work function, the electron affinity (EA) of MoS_2 is shown in the red dash line.